Effects of Three-Dimensional Electromagnetic Structures on Resistive-Wall-Mode Stability of Reversed Field Pinches

F. Villone,[1] Y. Q. Liu,[2] R. Paccagnella,[3] T. Bolzonella,[3] and G. Rubinacci[4]

[1]*Ass. Euratom/ENEA/CREATE, DAEIMI, Universitá di Cassino, Via Di Biasio 43, 03043, Cassino, Italy*
[2]*EURATOM/UKAEA Fusion Association, Culham Science Centre, Abingdon, Oxon, OX14 3DB, United Kingdom*
[3]*Consorzio RFX, Ass. Euratom/ENEA, and C.N.R., Corso Stati Uniti 4, 35127, Padova, Italy*
[4]*Ass. Euratom/ENEA/CREATE, DIEL, Universitá di Napoli Federico II, Via Claudio 21, 80125, Napoli, Italy*
(Received 25 January 2008; published 25 June 2008)

In this Letter, the linear stability of the resistive wall modes (RWMs) in toroidal geometry for a reversed field pinch (RFP) plasma is studied. Three computational models are used: the cylindrical code ETAW, the toroidal MHD code MARS-F, and the CARMA code, able to take fully into account the effects of a three-dimensional conducting structure which mimics the real shell geometry of a reversed field pinch experimental device. The computed mode growth rates generally agree with experimental data. The toroidal effects and the three-dimensional features of the shell, like gaps, allow a novel interpretation of the RWM spectrum in RFP's and remove its degeneracy. This shows the importance of making accurate modeling of conductors for the RWM predictions also in future devices such as ITER.

DOI: 10.1103/PhysRevLett.100.255005 PACS numbers: 52.35.Py, 28.52.Av, 52.55.Fa, 52.65.Kj

Introduction.—Resistive Wall Modes (RWMs) are kink-like instabilities which grow on the time scale of magnetic field penetration through the metal structures surrounding a toroidal fusion plasma. This happens when these structures are close enough to the plasma, so that an ideally conductive wall would have stabilized the kink mode [1]. These branches of magneto-hydro-dynamic (MHD) modes have received, in recent years, an increasing attention in fusion plasma physics research, in view of the steady state operations of future thermonuclear devices such as the International Tokamak Experimental Reactor (ITER). In ITER advanced scenarios, in particular, the RWM instability will set the most stringent limit to the plasma performance in terms of the stored internal kinetic energy and hence to its operational space [2]. For this reason, it is of fundamental importance to make reliable predictions about the RWM stability boundary and the so-called beta limits. However, some open issues still remain in RWM modeling. One is the estimate of the stabilization effects due to plasma rotation and dissipation [3]. Another is the evaluation of the effects of the complex three-dimensional conducting structures surrounding the plasma.

We study RWM stability in a reversed field pinch (RFP). Tokamaks and RFP devices share many common features of the RWM physics and its active control. In RFPs, however, RWMs are nonresonant current driven instabilities [4], generally not affected by dissipation and flow. This removes one of the modeling uncertainties mentioned above. As a consequence, the RWMs in RFPs are very reproducible and their growth rates, given a fixed geometry of the passive structure, is well determined by standard single-fluid MHD. For this reason, RFPs are a very interesting test bed for numerical MHD codes calculating the RWMs stability and control. Such codes, once validated, can be used to make predictions and estimations on other devices like tokamaks.

In this paper we focus on the RFX-mod experiment [5] which has a major radius R of 2 m, a plasma minor radius a of 0.459 m and a stabilizing copper shell at minor radius 0.513 m, of width 3 mm and a vertical field penetration time around 55 ms. This shell is made of four pieces, two of the gaps are left insulated, while the other two are short circuited as reported in the following. Moreover, an overlapping region is present corresponding to the insulated poloidal gap. Outside this shell there is another conducting structure, for mechanical purposes, on which a set of 192 saddle coils for feedback control are mounted, 4 at each of 48 equally spaced toroidal locations. Inside the shell a vacuum vessel, with short penetration time of 1–2 ms, is also present. Because of the complex geometry of conductors surrounding the plasma, in addition to the ETAW cylindrical code [6] and to the MARS-F toroidal code with axisymmetric walls [7], it has been necessary to apply a new computational tool, called CARMA [8,9], able to rigorously take into account the three-dimensional details of the conducting structures in the solution of the plasma stability problem.

We report a comparison of the RWM growth rates predicted by the various computational models and experimental evidence, showing a good agreement and suggesting motivations for possible discrepancies between cylindrical theory and experiments. Indeed, toroidal and 3D effects allow a new understanding of RWM spectrum in RFP's. In particular, three-dimensional electromagnetic effects may play a significant role in RWM stability. This has a direct implication to ITER predictions.

Modeling tools.—We make a Fourier decomposition of all quantities in the toroidal and poloidal direction; let us call m and n the poloidal and the toroidal mode numbers.

The cylindrical code ETAW has been extensively used for RFP calculations [10]. The code solves the linear cylindrical resistive incompressible MHD equations, using a spectral formulation and a matrix shooting eigenvalue scheme. The problem is solved in presence of up to two resistive walls, where thin shell boundary conditions are specified. The plasma model is solved inside the first wall and the solution is then matched to the external solution of the vacuum cylindrical Laplace equation, analytically known in terms of modified Bessel Functions.

MARS-F is a stability code that solves single-fluid MHD equations [7]. The code also includes a vacuum region, thin conducting shells, and feedback coils. Other features of the code, such as sheared toroidal plasma rotation, sound wave or kinetic damping terms, are not included in the simulations in this Letter. The major limitation of the code is that it can only treat conducting structures (walls or coils) that are axisymmetric along the major axis of the torus. This is because the code assumes a $\exp(jn\phi)$ variation of the eddy currents in these conductors along the toroidal angle ϕ.

CARMA is a recently developed code [8,9], able to analyze RWMs taking rigorously into account the three-dimensional features of the conducting structures surrounding the plasma. For a given toroidal mode number n, the linearized single-fluid MHD equations are solved inside a suitable coupling surface S, in between the plasma and the conducting structures. Neglecting plasma mass (which is an excellent approximation on typical RWM time scales), the instantaneous plasma response matrix to magnetic field perturbations on S are computed, using MARS-F. Such plasma response matrix is coupled to a 3D volumetric integral formulation of the eddy currents problem, which describes the conducting structures by means of a three-dimensional finite elements mesh. The CARMA code has been successfully benchmarked with MARS-F and applied to ITER [8,9].

Numerical and experimental results.—Usually, the problem of finding the RWM growth rates is studied in RFX-mod in the cylidrical limit since this has been shown [6] to be a good approximation, due to the low safety factor q which characterizes the RFPs. This is a major difference with respect to the tokamak case, where the RWMs are strongly ballooning in the outboard torus region, due to the unfavorable curvature and high pressure. In addition, being nonresonant, the RWM modes in RFPs are generally not influenced by the plasma sub-Alfvenic flow [11]. This greatly simplifies the stability analysis and the comparison with the experiments.

In RFPs the spectrum of unstable Fourier modes is dominated by the $m = 1$ poloidal harmonic in a wide range of n's values. Indeed, in the cylindrical limit, it is possible to consider each (m, n) mode as evolving separately. This leads to an assumption that the $(1, n)$ mode may have a different growth rate with respect to the $(-1, n)$ mode (which is the same as the $(1, -n)$ mode)—one of the two can even be stable. In the present context, toroidal coupling does not allow us to make this assumption: for a given n value, only "global" modes can occur, involving theoretically all m harmonics (although a few of them may be dominant). In cases where both $(1, n)$ and $(1, -n)$ cylindrical modes are unstable, they merge to two (or more, for reasons discussed in the following) unstable toroidal modes with the same n number but generally different growth rates. Being toroidal effects expected to be small, the growth rates of these merged modes are close to those computed in the cylindrical limit.

First, we assume an axisymmetric shell—although described in CARMA by a three-dimensional finite elements mesh. This allows a direct comparison of the results of the three previously mentioned codes. The equilibrium profile is characterized by the values $F = -0.136$ and $\Theta = 1.49$, where Θ (resp. F) is the ratio between the poloidal (resp. toroidal) field at the plasma boundary and the section averaged toroidal field, and has been reconstructed following the parametrization of the $\alpha - \theta_0$ model, widely used also to describe experimental data, in the zero pressure limit [6].

Table I reports the growth rates of the unstable RWMs as predicted by the three codes. The agreement is satisfactory; the small discrepancies are due to the different numerical treatment of conducting and vacuum regions in CARMA and MARS-F. For $n = 2$ and $n = 3$ two unstable global modes are found by MARS-F and CARMA, corresponding to the $m = 1$ and $m = -1$ modes of the cylindrical limit. CARMA uses the plasma response matrices computed for $n = 1 \ldots 6$, both one at a time (monomodal response) and all together (multimodal response). The eigenvalues of the monomodal and of the multimodal response are identical, as expected with an axisymmetric wall. For each unstable eigenvalue of MARS-F and of ETAW, CARMA finds in fact a pair of coinciding unstable eigenvalues; these correspond to two eigenvectors which are identical, except a shift of $\pi/(2n)$ in the toroidal direction. The two can be identified as $+n$ and $-n$ modes in MARS-F, which are identical with an axisymmetric equilibrium and wall geometry.

Figure 1 reports a comparison of the results predicted by MARS-F (close to the other codes with an axisymmetric shell) with experimental data of RFX-mod, as a function of the profile parameter F. The Θ value is fixed at 1.49 for all calculations. For this range of F, the experimental Θ value varies between 1.44 and 1.49. When multiple unstable

TABLE I. Growth rates with a 2D shell (results in s^{-1}).

n value	Cylindrical	MARS-F	CARMA
1	<0	<0	<0
2	<0	0.434	0.368
	2.45	1.81	1.94
3	1.82	2.08	1.91
	1.90	2.16	2.49
4	4.09	4.04	4.27
5	6.81	6.89	7.45
6	11.8	11.7	12.9

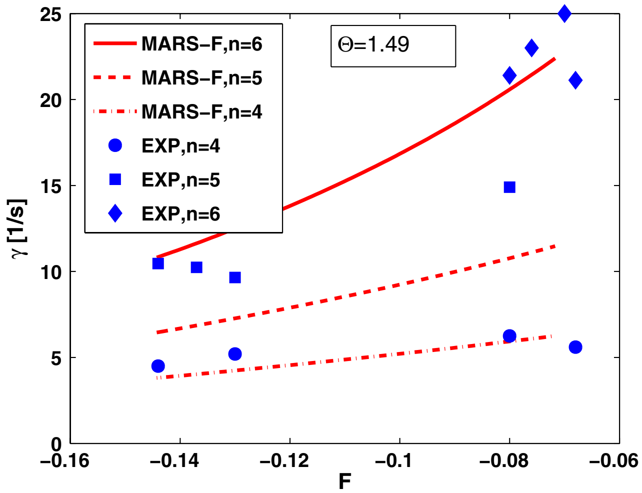

FIG. 1 (color online). Comparison with experimental growth rates.

modes are present, only the highest growth rate is reported. Evidently, the agreement is qualitatively and quantitatively satisfactory, although a slight underestimation can be noticed, especially for the $n = 5$ mode. In addition, for $n = 6$ around $F = -0.13$, the experimental measurements give a growth rate of about 20 s^{-1}, which does not agree with the 2D wall simulation results.

We have also performed some computations with CARMA using a nonaxisymmetric shell, in which the gaps have been introduced. No overlapping of the shell at the gaps is taken into account. One of the poloidal gaps and the inner toroidal gap have been kept insulated, as it is done in RFX-mod (see Fig. 2). The other two gaps are short circuited on the device: the poloidal gap is welded, while the outer toroidal gap is short circuited by means of a number of copper plates [12]. Table II reports the growth rates when assuming that such short circuits are perfect, for

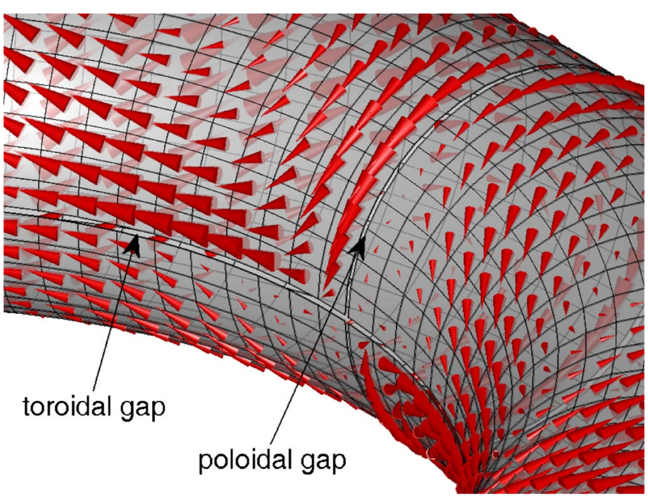

FIG. 2 (color online). Gaps location and current density distribution corresponding to one of the $n = 3$ unstable modes.

the same equilibrium of Table I. The shell current density distribution of one of the unstable $n = 3$ modes close to the gaps is reported in Fig. 2.

Comparing such results with those of Table I, we notice that the 3D effect of the gaps can lead to a sometimes significant increase of the growth rate. It should also be noted that by breaking the symmetry of the wall with the gaps, we remove the degeneracy of the spectrum, giving rise to pairs of eigenvalues which are close each to the other, but not coinciding any more.

The two pairs of unstable eigenvalues, reported in Table II for $n = 3$, are the counterpart, in toroidal 3D geometry, of the two pairs of unstable eigenvalues found for this equilibrium in the cylindrical limit: $(1, n)$, $(-1, -n)$ and $(1, -n)$, $(-1, n)$. Similar considerations apply to the four unstable eigenvalues obtained for $n = 2$, although in this case the two marginally unstable modes are in fact stable in the cylindrical limit.

In addition, we observe that the eigenvalues of the multimodal response are not exactly coinciding with those of the monomodal response. This is due to the fact that a nonaxisymmetric wall may couple, even in linear MHD, modes with different n's [13].

Reexaming Fig. 1, we notice that such 3D effects tend to compensate the slight underestimation that the axisymmetric models give with respect to experimental values. For instance, the $n = 5$ growth rate increases of about 40%, up to around 10 s^{-1}, much closer to experimental values. However, it should be noted that the introduction of additional conducting structures (vessel and mechanical structures, neglected in the present study) could slow down again the estimated growth rate. This consideration applies obviously also to the cylindrical and axisymmetric computations reported above.

TABLE II. Growth rates predicted by CARMA with a 3D shell with gaps (results in s^{-1}).

n value	CARMA monomodal	CARMA multimodal
1	<0	<0
2	0.447	0.448
	0.459	0.462
	2.40	2.33
	2.48	2.36
3	2.58	2.61
	2.62	2.64
	2.96	3.13
	3.04	3.26
4	5.46	5.63
	5.53	5.78
5	9.62	9.91
	9.73	10.2
6	17.0	17.6
	17.2	18.2

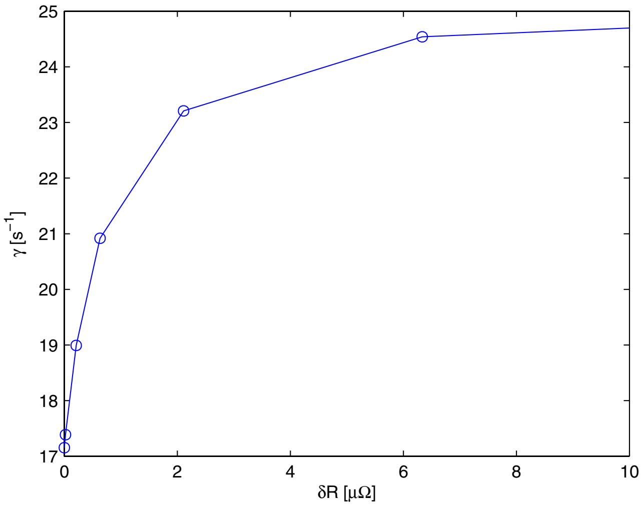

FIG. 3 (color online). Growth rate of the $n = 6$ mode predicted by CARMA as a function of additional resistance at the outer toroidal gap.

In order to get a deeper insight on 3D effects, the short circuited gaps have been represented in CARMA by a contact resistance, with the same technique used in [14]. Figure 3 reports the monomodal $n = 6$ growth rate assuming that the second poloidal gap is perfectly short circuited and representing the outer toroidal gap as an increasing contact resistance δR. The case $\delta R = 0$ corresponds to the results presented in Table II.

Evidently, a value δR of a few $\mu\Omega$ accounts for an increase of the growth rate up to around 50%. Conversely, the poloidal gap has a less important effect, giving rise to variations of the order of 10% at most. However, in RFX-mod the contact resistance of the toroidal gap has been estimated as being $<0.5\ \mu\Omega$ [15], so this effect can possibly justify a further increase of the growth rate up to around 20 s^{-1}. This value is in better agreement with experiments than purely axisymmetric estimates.

Conclusions and perspective.—Resistive wall modes occurring in RFX-mod have been studied with a number of computational tools. Specifically, the application of the MARS-F and CARMA codes allows the analysis of RWMs including toroidal effects, multimodal plasma evolution and three-dimensional features of the conducting structures surrounding the plasma. In particular, the inclusion of toroidal effects allows a new understanding of RWM spectrum of RFP devices, and 3D effects are shown to remove the spectrum degeneracy and to cause multimodal coupling even in the linear case. All these features allow a successful prediction of experimental growth rates, that are often substantially underestimated when such effects are not taken into account. This comparison was made possible by the fact the RWMs in RFPs are highly reproducible, being nonresonant current driven modes, while it would be much harder to achieve on other devices.

Several points deserve further attention. First of all, a more realistic description of the electromagnetic structures should be given, including features neglected in this Letter, like for instance the vessel and the mechanical structure, which are expected to play (especially the second) a stabilizing role. Second, a thorough comparison with experimental data will be done, trying to test the sensitivity of the stability results on variations of the plasma equilibrium. Indeed, it has been already shown [16] that the growth rate of the first on-axis nonresonant mode can be affected by uncertainties of the safety factor profile near the magnetic axis.

F. Villone and G. Rubinacci gratefully acknowledge useful discussions with Professor R. Albanese and Dr. A. Portone and the help of Dr. M. Cavinato for providing the geometrical data of RFX-mod. R. Paccagnella and T. Bolzonella thank the RFX-team. Y. Q. Liu thanks M. S. Chu and S. C. Guo for modifying CHEASE for computing RFP equilibria. This work was supported in part by Italian MIUR under PRIN grant and by Consorzio CREATE.

[1] J. P. Goedbloed *et al.*, Nucl. Fusion **12**, 649 (1972).
[2] Y. Q. Liu *et al.*, Nucl. Fusion **44**, 232 (2004).
[3] A. Bondeson and D. J. Ward, Phys. Rev. Lett. **72**, 2709 (1994).
[4] T. C. Hender *et al.*, Nucl. Fusion **29**, 1279 (1989).
[5] P. Sonato *et al.*, Fusion Eng. Des. **66**, 161 (2003).
[6] R. Paccagnella *et al.*, Nucl. Fusion **31**, 1899 (1991).
[7] Y. Q. Liu *et al.*, Phys. Plasmas **7**, 3681 (2000).
[8] F. Villone *et al.*, 34th EPS Conference Warsaw (2007) P5.125.
[9] R. Albanese *et al.*, IEEE Trans. Magn., **44**, 1654 (2008).
[10] R. Paccagnella, Nucl. Fusion **38**, 1067 (1998).
[11] S. C. Guo *et al.*, Phys. Plasmas **6**, 3868 (1999).
[12] W. Baker *et al.*, Fusion Eng. Des. **63–64**, 461 (2002).
[13] R. Fitzpatrick, Phys. Plasmas **1**, 2931 (1994).
[14] F. Villone, IEEE Trans. Magn. **36**, 1706 (2000).
[15] G. Marchiori, personal communication, Dec. 2007.
[16] R. Paccagnella *et al.*, Nucl. Fusion **47**, 990 (2007).